Catalysis Today 179 (2012) 85–90

Contents lists available at ScienceDirect

Catalysis Today

journal homepage: www.elsevier.com/locate/cattod

High activity of iron containing metal–organic-framework in acylation of *p*-xylene with benzoyl chloride

Lenka Kurfiřtová[a], You-Kyong Seo[b], Young Kyu Hwang[b], Jong-San Chang[b], Jiří Čejka[a,*]

[a] *J. Heyrovský Institute of Physical Chemistry, Academy of Sciences of the Czech Republic, v.v.i., Dolejškova 3, CZ-182 23, Prague 8, Czech Republic*
[b] *Research Group for Nanocatalyst, Korea Research Institute of Chemical Technology, Catalysis Centre for Molecular Engineering, Taejon 305600, South Korea*

ARTICLE INFO

Article history:
Received 30 June 2011
Received in revised form 29 July 2011
Accepted 2 August 2011
Available online 9 September 2011

Keywords:
Acylation
p-Xylene
Benzoyl chloride
Zeolites
Metal–organic-frameworks
MIL-100(Fe)

ABSTRACT

Catalytic behavior of metal–organic-frameworks (MOFs) $Cu_3(BTC)_2$, MIL-100(Fe) and MIL-100(Cr) was investigated in *p*-xylene acylation with benzoyl chloride and compared with the behavior of large pore zeolites Beta and USY. It has been clearly shown that MIL-100(Fe) exhibit much higher conversion of benzoyl chloride with excellent selectivity in *p*-xylene acylation. The performance of MIL-100(Fe) catalyst was favorable with those of other conventional heterogeneous catalysts like zeolites. Conversion of benzoyl chloride equal to 100% was achieved over MIL-100(Fe) with 20–30 min under optimized reaction conditions. It is assumed that unsaturated Lewis acid sites associated with the presence of Fe exhibit optimum acid strength for catalyzing this acylation reaction.

1. Introduction

Alkyl–aryl and aryl–aryl ketones represent important groups of organic compounds with a broad range of applications as intermediates or final products in pharmaceutical or perfume industry. The formation of these ketones is mainly performed using Friedel–Crafts acylations of aromatic compounds. However, traditional homogeneous Friedel–Crafts catalysts like $AlCl_3$, BF_3 and H_2SO_4 involve serious problems with separation and recovery, disposal of spent catalyst, corrosion, and high toxicity. The disadvantages of homogeneous catalysts can be overcome using heterogeneous catalysts like zeolites including two-dimensional ones, metal–organic-frameworks or mesoporous molecular sieves [1–4]. Recently, different structural types of molecular sieves have been evidenced to catalyze acylations of aromatic compounds, for example, anisole [5] veratrole [6], 2-methoxynaphthalene [7], ferrocene [8] or naphthalene [9]. The success of zeolites for acylation reactions was evidenced by Rhodia company in a commercial application of zeolites Beta and Y for acylation of anisole and veratrole with acetic anhydride [6]. Numerous papers published on acylation ability of zeolites resulted in a better understanding of their key chemical and textural parameters including tuned acidity, controlled site density, high thermal and hydrothermal stability, and shape selectivity towards reactants, products, and restricted transition states [10]. While zeolites are well-established and mature catalysts for fine chemical synthesis with still limited pore sizes to about 1 nm, mesoporous molecular sieves show some potential, and metal–organic-frameworks represent novel type of materials with not yet completely understood properties and recognized potential, particularly in catalysis [11].

Metal–organic-frameworks (MOFs) are hybrid organic–inorganic molecular sieves with tremendous opportunities to tailor their pore sizes, their shapes as well as dimensionality [12,13]. In addition, chemical environment can be finely controlled by combining appropriate building blocks, including metal species (metals, oxide, etc.) with organic linkers. Porous copper trimesate, $Cu_3(BTC)_2$ (known as HKUST-1, BTC = benzene-1,3,5-tricarboxylate) [14], is a rigid MOF with a zeolite-like structure and free coordination sites on the Cu^{2+} ion. It consists of main channels of a square cross-section of ca. 0.9 nm diameter and tetrahedral side pockets of ca. 0.5 nm, which are connected to the main channels by triangular windows of ca. 0.35 nm diameter. MIL-100(Fe) [15] and MIL-100(Cr) [16] are the isomorphous cubic metal(III) trimesates with giant pores. The crystalline iron(III) trimesate MIL-100(Fe) is commonly built up from oxo-centered trimers of iron(III) octahedra (three iron(III) octahedra sharing a common vertex of μ_3-O) with terminal ligands (F/OH, H_2O). In the as-synthesized form, in the terminal position of the octahedra of the iron trimer there are two H_2O molecules and, depending on the synthesis conditions, either F^- or OH^- anions. Their

* Corresponding author.
E-mail address: Jiri.cejka@jh-inst.cas.cz (J. Čejka).

0920-5861/$ – see front matter © 2011 Elsevier B.V. All rights reserved.
doi:10.1016/j.cattod.2011.08.001

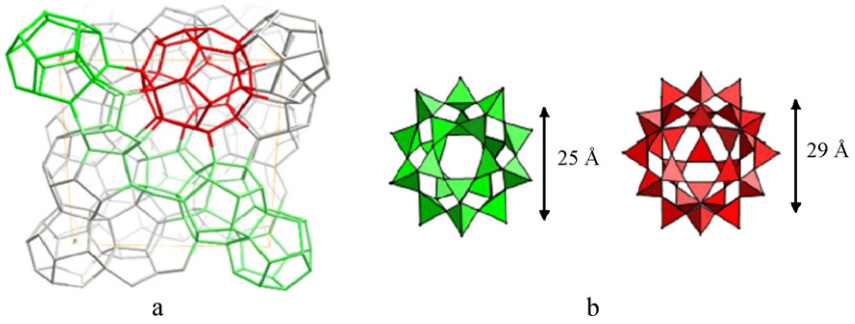

Scheme 1. (a) Schematic view of one unit cell of MIL-100(Fe) and (b) two types of mesoporous cages in polyhedral mode of MIL-100 (Fe).

linkages to the rigid trimesate (1,3,5-benzenetricarboxylate) ligand generate microporous super-tetrahedral units. The structure has a cubic array of very large pores (2.5–2.9 nm) accessible through microporous windows (0.47–0.86 nm) with a large BET surface area (>2000 $m^2\ g^{-1}$). The structure of MIL-100(Fe), the most active MOF catalysts in this study, is provided schematically in Scheme 1.

It is expected that MOFs can be efficient catalysts particularly in liquid phase reactions being performed at temperatures up to 150 °C as their thermal stability under reaction conditions is usually limited. Many examples of reactions catalyzed by MOFs have been recently reported in the literature [11] including acylations [15], cyanosilylations [17], oxidations [18,19], condensations [20,21], etc. Mostly, different MOF catalysts exhibit high conversions and selectivities, however, without reporting on the comparison with conventional heterogeneous catalysts.

This contribution focuses on the acylation of *p*-xylene with benzoyl chloride over MOFs (MIL-100(Fe), MIL-100(Cr), and $Cu_3(BTC)_2$) and on the comparison of their behavior with large pore zeolites Beta and USY. The effects of the type of acid site, activation procedure, reaction conditions and molar ratio between acylating agent and substrate on the course of the reaction were investigated.

2. Experimental

2.1. Chemicals

p-Xylene and benzoyl chloride (Sigma–Aldrich) were used without any treatment.

2.2. Catalysts

Zeolites Beta and USY with different Si/Al ratio were investigated as catalysts (for their provenience and properties, see Table 1).

$Cu_3(BTC)_2$ was synthesized by microwave method using a solution of copper sulfate trihydrate ($Cu(SO_4)_2{\cdot}3H_2O$), BTC and ethylene glycol as solvent similarly as described elsewhere [22]. MIL-100(Fe) was prepared from hydrothermal reaction of BTC with metallic iron, HF, nitric acid and H_2O at 150 °C for 8 h, as reported elsewhere [23]. MIL-100(Cr) was hydrothermally synthesized at 220 °C for 8 h according to the previous method [15].

2.3. Characterization

For zeolites Beta and USY, the concentration and type of acid sites were determined by adsorption of d_3-acetonitrile as probe molecule followed by FTIR spectroscopy (Nicolet Protégé 460) using the self-supported wafer technique. The concentrations of Lewis and Brønsted acid sites in the samples were calculated with the extinction coefficients (for d_3-acetonitrile $\varepsilon(B) = 2.05 \pm 0.1$ cm μmol^{-1}, $\varepsilon(L) = 3.6 \pm 0.2$ cm μmol^{-1}, pyridine $\varepsilon(B) = 1.67 \pm 0.1$ cm μmol^{-1}, $\varepsilon(L) = 2.22 \pm 0.1$ cm μmol^{-1}) [24].

Determination of the concentrations of Lewis acid sites in MOFs under study is much more complex problem. Pyridine was used for this purpose and it looks that the average value for MIL-100(Fe) is approx. 2.0 mmol/g after activation around 180–200 °C in vacuo [25]. The adsorption and localization of water in MOF materials is currently under detailed experimental and theoretical investigations (e.g. [26]). A detailed study is currently in progress.

The shape and size of zeolite crystallites were determined by scanning electron microscopy (Jeol, JSM-5500LV). The crystallinity of zeolites was determined by X-ray powder diffraction with Bruker D8 X-ray powder diffractometer equipped with a graphite monochromator and position-sensitive detector using Cu Kα radiation in the Bragg–Brentano geometry. Textural properties of zeolites and studied were determined with a Micromeritics ASAP 2020 volumetric instrument at −196 °C. The activation of these materials was carried out at 150 °C for and 300 °C for zeolites while for other details, see Ref. [27]. In the case of MOF catalysts, X-ray powder diffraction patterns of all the samples were recorded by a Rigaku diffractometer (D/MAX IIIB, 2 kW) using Ni-filtered Cu Kα-radiation (40 kV, 30 mA, λ = 1.5406 Å) and a graphite crystal monochromator. BET specific surface areas of catalysts were measured by N_2 physisorption isotherms at −196 °C using a sorption analyzer (Micromeritics, Tristar 3000) and standard multipoint BET analysis method. Samples were degassed in flowing N_2 for 5 h at 150 °C before N_2 physisorption measurements. The specific surface areas were evaluated using

Table 1
Characteristics of MOFs and zeolites used in this study.

Catalyst	Origin	Channel structure	Channel diameter (nm)	Surface area ($m^2\ g^{-1}$)	Si/Al ratio
Beta	Zeolyst	3D	0.64 × 0.76	674	12.5
			0.56 × 0.56	642	37.5
USY	Zeolyst	3D	0.74	769	15
				774	40
$Cu_3(BTC)_2$		3D	0.35, 0.50, 0.90	1720	n.a.
MIL-100(Fe)	MTN[a]	3D	0.47 × 0.55, 0.86	2050	n.a.
MIL-100(Cr)	MTN	3D	0.47 × 0.55, 0.86	1980	n.a.

[a] Zeolite structural code.

the Brunauer–Emmett–Teller (BET) method in the p/p_0 range of 0.05–0.2.

2.4. Catalytic test

Acylation of *p*-xylene with benzoyl chloride was investigated in a liquid phase under atmospheric pressure at the reaction temperatures between 80 and 130 °C in a multi-experimental work station StarFish (Redleys Discovery Technologies, UK). The reactions were performed in a 50 ml round bottom flask equipped with a condenser. In a typical experiment, 97 mmol of *p*-xylene, 16 mmol of benzoyl chloride, 0.5 g of dodecane (internal standard) and 0.2 g of catalyst were used. The zeolite catalysts were activated by heating at 450 °C for 90 min with a temperature rate 10 °C/min while MOF catalysts at 130–200 °C (standard temperature of activation = 150 °C with a temperature rate 2 °C/min) for 90 min. The amount of catalyst was varied between 0.1 and 0.4 g and molar ratio of *p*-xylene to benzoyl chloride from 8:1 to 2:1.

Typical reaction was carried out as follows: activated catalyst, internal standard, substrate were introduced in the flask, stirred and heated. Acylating agent was added into the vessel with a syringe when the desired reaction temperature was reached.

Samples of the reaction mixture were taken periodically from the reaction vessel and analyzed by a gas chromatography (Agilent 6850) using nonpolar DB-5 column (length 20 m, diameter 0.180 mm, film thickness 0.18 μm). Reaction products were identified using mass spectrometry (ThermoFinnigan, FOCUS DSQ II Single Quadrupole GC/MS).

3. Results and discussion

3.1. Characterization

Zeolites Beta/12.5, USY/15, and USY/40 were evaluated for the crystallinity using X-ray powder diffraction (not shown here) confirming clear evidence of the high crystallinity and phase purity. The size of the crystallites was determined from SEM images, while showing that zeolite Beta exhibits small crystals of about 0.1–0.2 μm, zeolites USY possess crystals around approximately 0.6 μm.

Acidic properties of zeolites, namely type and concentrations of Brønsted and Lewis acid sites were assessed using d_3-acetonitrile. All three zeolites exhibit characteristic absorption band at about 3740–3745 cm^{-1} being assigned to the silanol OH groups. The interaction of this band with d_3-acetonitrile is rather weak not changing the intensity of this band after adsorption of d_3-acetonitrile. The absorption bands of acidic bridging OH groups appear at 3610 cm^{-1} for zeolite Beta and at 3565 and 3630 cm^{-1} for USY zeolites [28,29]. Adsorption of d_3-acetonitrile removed these bands while new bands appeared in the region 2250–2350 cm^{-1}. The absorption band around 2300 cm^{-1} is due to the interaction of d_3-acetonitrile with Brønsted acid sites while new band around 2325 cm^{-1} is characteristic of the d_3-acetonitrile on Lewis acid site. The concentrations of individual Brønsted and Lewis acid sites (using extinction coefficients from Ref. [24]) are provided in Table 2.

Table 2
Concentrations of Brønsted and Lewis acid sites of zeolites under study, determined from adsorption of d_3-acetonitrile followed by FTIR spectroscopy.

Zeolite	C_{Lc} (mmol/g)	c_{Bc} (mmol/g)
Beta/12.5	0.39	0.14
Beta/37.5	0.11	0.17
USY/15	0.34	0.20
USY/40	0.04	0.02

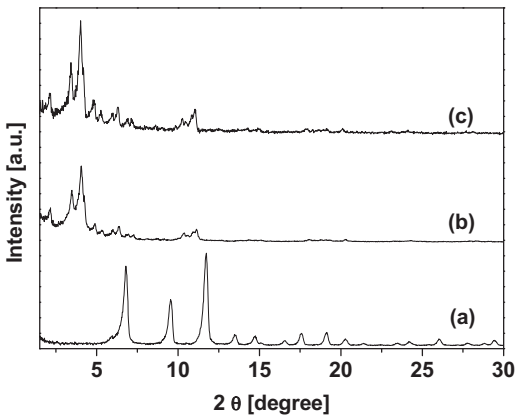

Fig. 1. XRD patterns of metal–organic frameworks (a) $Cu_3(BTC)_2$, (b) MIL-100(Cr) and (c) MIL-100 (Fe).

Fig. 1 shows typical XRD patterns of the as-synthesized MOFs such as $Cu_3(BTC)_2$, MIL-100(Cr) and MIL-100(Fe). To confirm the permanent porosity, we obtained N_2 physisorption isotherms of the MOFs at −196 °C after evacuation at 150 °C for 12 h (Fig. 2). $Cu_3(BTC)_2$ showed a type I isotherm, which adsorbs the large amount of N_2 at relatively low pressure. In the case of MIL-100(Fe) and MIL-100(Cr), the adsorption isotherm was between type I and type IV with two point uptakes at $p/p_0 = 0.06$ and 0.12 corresponding to the micropore windows and mesopore cages as previously described [16]. From fitting the BET equation between $p/p_0 = 0.05$ and 0.2 to the resulting N_2 isotherm, the BET surface areas of $Cu_3(BTC)_2$, MIL-100(Cr) and MIL-100(Fe) are 1720 $m^2\ g^{-1}$, 1980 $m^2\ g^{-1}$, and 2050 $m^2\ g^{-1}$, respectively.

3.2. Catalysis

p-Xylene acylation with benzoyl chloride was used in this study from two main reasons: (i) primary product of this acylation reaction is always 1-benzoyl-2,5-dimethyl benzene and all other possible products are formed by competitive or subsequent reactions; (ii) the primary product is relatively bulky, thus, size of the channels can play a substantial role in the acylation reaction.

Fig. 3 provides the time-on-stream dependence of benzoyl chloride conversion over different zeolites and metal–organic-framework catalysts. While only slight differences were observed for zeolites Beta and USY, MOF catalysts exhibited very

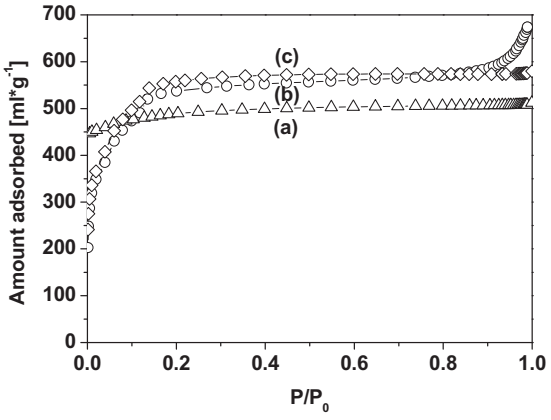

Fig. 2. N_2 physisorption isotherms of MOFs: (a) $Cu_3(BTC)_2$, (b) MIL-100(Cr) and (c) MIL-100 (Fe).

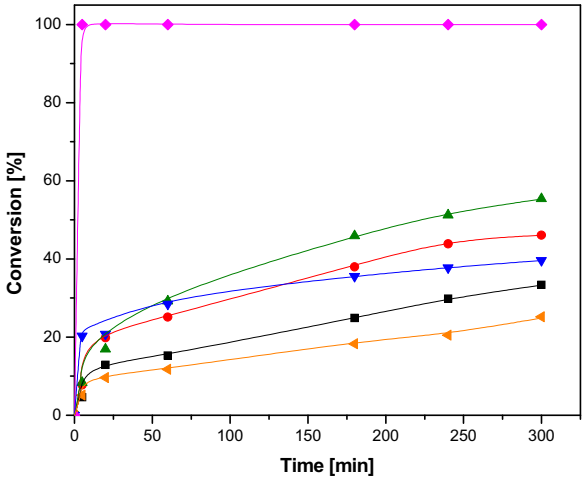

Fig. 3. Time-on-stream behavior of different zeolites and MOF catalysts in *p*-xylene benzoylation; benzoyl chloride conversion over Beta/12.5 (■); USY/15 (●); USY/40 (▲); $Cu_3(BTC)_2$ (▼); MIL-100(Fe) (◆); MIL-100(Cr) (◀) (activation temperature 130 °C).

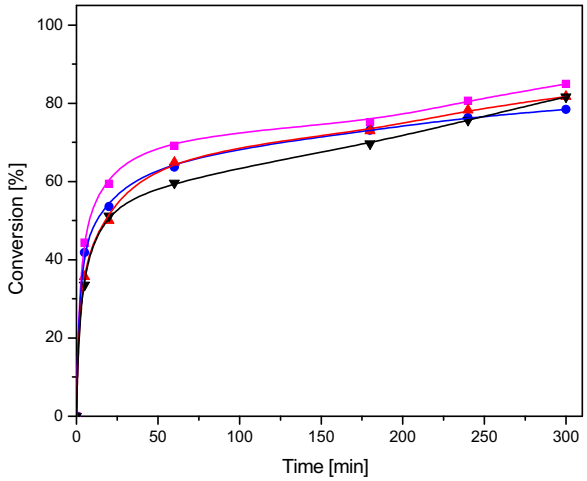

Fig. 4. Time-on-stream dependence of benzoyl chloride conversion over MIL-100(Fe) in *p*-xylene benzoylation for different activation temperatures; 130 °C (■); 150 °C (●); 170 °C (▲); 200 °C (▼).

different conversions of benzoyl chloride. In the case of zeolites, conversions of benzoyl chloride increase in the order Beta/12.5 < USY/15 < USY/40 (Fig. 1). It indicates that both channel size of zeolites as well as concentration of acid sites influence the resulting conversion. Channels of USY zeolites are slightly larger than those of Beta (Table 1) and conversion of benzoyl chloride increases with decreasing concentration of acid sites. It can be inferred that adsorption/desorption equilibrium is playing a substantial role in this reaction. Similar finding was observed also for other acylation reactions, e.g. [9]. In contrast to the catalytic behavior of zeolites Beta and USY, substantial differences in benzoyl chloride conversion were achieved over individual MOF catalysts. The lowest conversion during the whole kinetic run was obtained over MIL-100(Cr) reaching about 20% after 300 min. $Cu_3(BTC)_2$ exhibited a higher conversion than zeolite Beta being 37% against 31%, respectively. The highest conversion was obtained over MIL-100(Fe). In this case, benzoyl chloride conversion reached 100% within about 15 min of the reaction. This excellent conversion over MIL-100(Fe) can be probably attributed to the presence of Lewis acid sites connected with Fe in the framework of this MOF catalyst. It is well known that acylation reactions can be catalyzed by both Brønsted as well as Lewis acid sites [1,2]. While no Brønsted sites are reported as for MIL-100(Fe), it is expected that Fe-Lewis sites are responsible for the catalytic activity. After activation in vacuo, the amount of Lewis sites determined from pyridine adsorption was about 2.0 mmol/g [25]. On the other hand, it is still questionable if also other Fe species can catalyze the acylation reaction. The analysis of filtrate after the reaction did not show any observable amount of iron, which could evidence that the activity of MIL-100(Fe) is bound to the heterogeneous material.

Based on the fact that substantially different conversions of benzoyl chloride were achieved over individual MOF catalysts, for further investigations of the effect of activation, catalyst amount and ratio of reactants, we chose the reaction temperature 80 °C for MIL-100(Fe) and 130 °C for $Cu_3(BTC)_2$ and MIL-100(Cr).

Over all catalyst investigated, the selectivity towards the primary acylation product, 1-benzoyl-2,5-dimethylbenzene, was 100%. This evidences that under the reaction conditions applied no secondary reactions proceeded including a possible isomerization of *p*-xylene. This result is most probably influenced by some steric constraints on the primary acylation product and not a result of shape selectivity. Large cages inside MIL-100(Cr) and MIL-100(Fe) would allow the second acylation step, however, such products were not observed during our experiments (even at very low concentrations). As MIL-100(Fe) exhibited the highest conversion in *p*-xylene acylation with benzoyl chloride among other catalysts investigated, we studied the effect of activation temperature on the benzoyl chloride conversion. Fig. 4 shows that both initial reaction rates as well as final conversions of benzoyl chloride do not differ substantially. Benzoyl chloride conversion after activation at 130 °C for 300 min of the reaction was equal to 82% while the conversion over MIL-100(Fe) activated at 150 °C was about 77%. In the activation temperature range between 130 and 200 °C we did not find any straightforward relation between the benzoyl chloride conversion and temperature of activation. Thus, for further experiments we have chosen the activation of temperature equal to 150 °C to minimize the potential risk of structure degradation of the individual catalysts; also the activation prior to other characterization experiments was done at this temperature.

The effect of the amount of catalysts for all three MOF materials under study is provided in Fig. 5. In general, the order of the conversions of benzoyl chloride despite the amount of catalyst used is MIL-100(Fe) > $Cu_3(BTC)_2$ > MIL-100(Cr). It should be noted that experiments reported in Fig. 5 were carried out at reaction temperature of 130 °C for $Cu_3(BTC)_2$ and MIL-100(Cr) while at 80 °C for MIL-100(Fe). The reaction temperature for acylation experiments over MIL-100(Fe) was decreased in order to decrease substantially the conversion of benzoyl chloride. Conversions of benzoyl chloride over MIL-100(Fe) at 130 °C reached 100% within 15–30 min. Thus, to properly compare the catalytic behavior at different amounts of catalysts, the reaction temperature was decreased. Even after the decrease in the reaction temperature to 80 °C the benzoyl chloride conversion was in the range of 65 (0.1 g) to 95 (0.4 g)% after 300 min of the reaction time (Fig. 3). In contrast, the conversion of benzoyl chloride over $Cu_3(BTC)_2$ reached only from 8% (the amount of catalyst equal to 0.1 g) up to 45% (0.4 g), Fig. 5, although the reaction was performed at 130 °C. Even lower conversions of benzoyl chloride were achieved over MIL-100(Cr), reaction temperature = 80 °C. In the case of the reaction performed with 0.1 g of the catalyst, only the conversion of benzoyl chloride achieved 7%. The highest conversion being 30% was reached using 0.4 g of MIL-100(Cr). These results clearly show the dominance of MIL-100(Fe) in catalyzing acylation of *p*-xylene over different MOF catalysts.

The effect of different molar ratios of *p*-xylene and benzoyl chloride on the benzoyl chloride conversion is provided in Fig. 6. The reactions were again performed at 130 °C for $Cu_3(BTC)_2$ and

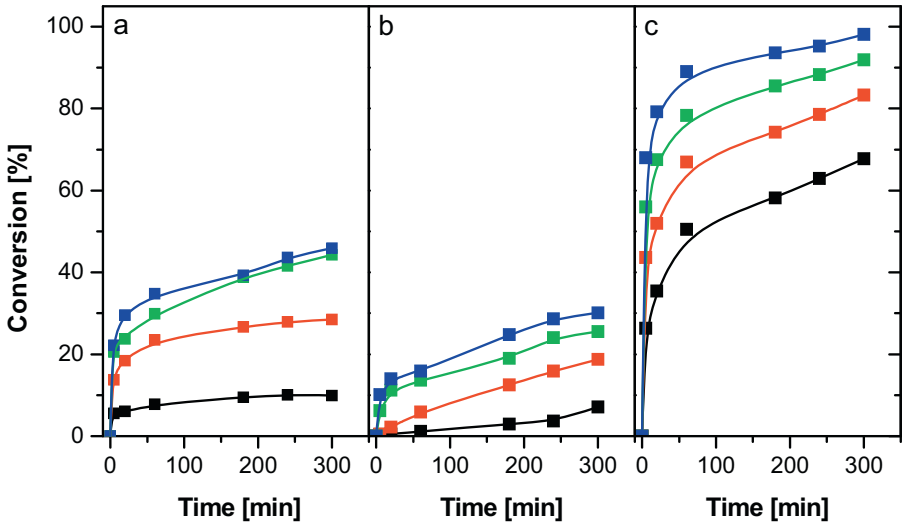

Fig. 5. Time-on-stream dependence of benzoyl chloride conversion over $Cu_3[BTC]_2$ (a), MIL-100(Cr) (b), and MIL-100(Fe) (c), in *p*-xylene benzoylation with different amount of catalysts; 0.1 g (■); 0.2 g (■); 0.3 g (■); 0.4 g (■), reaction temperature: $Cu_3[BTC]_2$ and MIL-100(Cr), 130 °C; MIL-100(Fe), 80 °C.

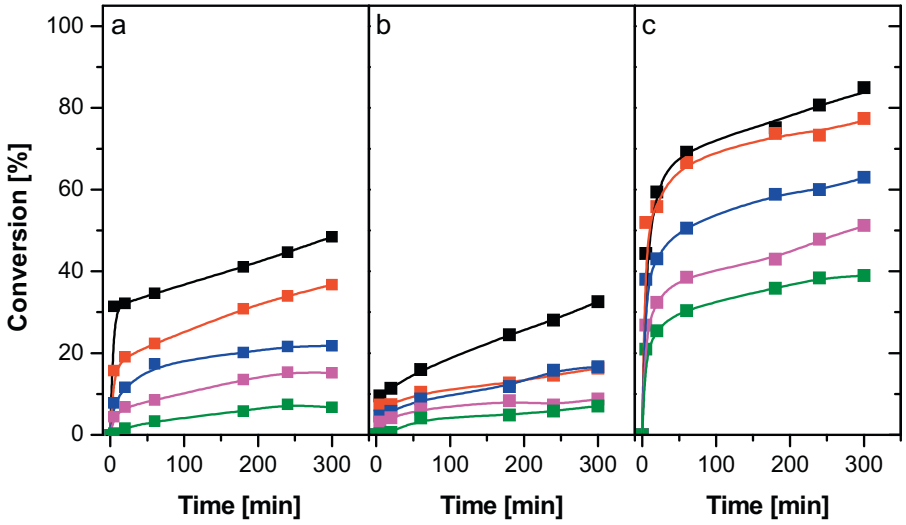

Fig. 6. Time-on-stream dependence of benzoyl chloride conversion over $Cu_3(BTC)_2$ (A), MIL-100(Cr) (B), and MIL-100(Fe) (C), in *p*-xylene benzoylation with different molar ratios *p*-xylene to benzoyl chloride; 8:1.0 (■); 8:2.0 (■); 8:2.5 (■); 8:3.4 (■); 8:4.0 (■); catalyst amount: 0.2 g; reaction temperature: $Cu_3[BTC]_2$ and MIL-100(Cr), 130 °C; MIL-100(Fe), 80 °C.

MIL-100(Cr) while at 80 °C MIL-100(Fe). Despite a much lower reaction temperature with MIL-100(Fe), conversions of benzoyl chloride were substantially higher than over $Cu_3(BTC)_2$ and MIL-100(Cr). Over all MOF catalysts used, the conversion of benzoyl chloride increased with increasing molar ratio of *p*-xylene to benzoyl chloride. The higher was the concentration of benzoyl chloride in the reaction mixture, the lower was the conversion, which quickly leveled off for longer reaction times. It strongly indicates the formation of adsorption/desorption equilibrium of reactants/products slowing down further reaction and preventing reaction completion. It is assumed that particularly benzoyl chloride is strongly bound to the unsaturated metal sites in individual MOF catalysts. This slows down the rate of diffusion and decreases thus conversion of benzoyl chloride. While the highest conversions of benzoyl chloride over $Cu_3(BTC)_2$ and MIL-100(Cr) reached 50 and 30% after 300 min of the reaction, respectively (reaction temperature = 130 °C), benzoyl chloride conversion over MIL-100(Fe) was above 80% although the reaction was carried out at 80 °C. Again, the results clearly evidence the superiority of MIL-100(Fe) catalyst for *p*-xylene acylation with benzoyl chloride.

4. Conclusions

p-Xylene acylation with benzoyl chloride was investigated using large-pore zeolites Beta and USY and different MOF catalysts. While zeolites Beta and USY exhibited similar conversions as $Cu_3(BTC)_2$ or MIL-100(Cr), the total conversions of benzoyl chloride were achieved over MIL-100(Fe). No secondary products were observed. Total yield of 1-benzoyl-2,5-dimethyl benzene was achieved over MIL-100(Fe) in the temperature range of 100–130 °C within 15–30 min of the reaction time. Activation temperature between 130 and 200 °C for MIL-100(Fe) was found to have a negligible role on the resulting conversion of benzoyl chloride.

Acknowledgements

The research leading to these results has received funding from the European Community's Seventh Framework Programme [FP7/2007-2013] under grant agreement no. 228862. LK and JČ acknowledge also the support of the Grant Agency of the Czech Republic (104/07/0383). Korean researchers acknowledge

the financial support by the international collaboration program (KICOS).

References

[1] G. Sartori, R. Maggi, Chem. Rev. 106 (2006) 1077–1104.
[2] M. Bejblová, D. Procházková, J. Čejka, ChemSusChem 2 (2009) 486–499.
[3] R.M. Martín-Aranda, J. Čejka, Top. Catal. 53 (2010) 141–153.
[4] W.J. Roth, J. Čejka, Catal. Sci. Technol. 1 (2011) 43–54.
[5] S.G. Wagholikar, P.S. Niphadkar, S. Mayadevi, S. Sivasanker, Appl. Catal. A 317 (2007) 250–257.
[6] C. Guignard, V. Pedron, F. Richard, R. Jacquot, M. Spagnol, J.M. Coustard, G. Perot, Appl. Catal. A 234 (2002) 79–90.
[7] M. Casagrande, L. Storaro, M. Lenarda, R. Ganzerla, Appl. Catal. A 201 (2000) 263–270.
[8] D. Procházková, M. Bejblová, J. Vlk, A. Vinu, P. Štěpnička, J. Čejka, Chem. Eur. J. 16 (2010) 7773–7780.
[9] L. Červený, K. Mikulcová, J. Čejka, Appl. Catal. A 223 (2002) 65–72.
[10] A. Corma, Chem. Rev. 95 (1995) 559–614.
[11] A. Corma, H. Garcia, F.X. Llabrés i Xamena, Chem. Rev. 110 (2010) 4606–4655.
[12] G. Férey, Chem. Soc. Rev. 37 (2008) 191–214.
[13] V. Calvino-Casilda, R.M. Martin-Aranda, Rec. Pat. Chem. Eng. 4 (2011) 1–16.
[14] S.S.-Y. Chui, S.M.-F. Lo, J.P.H. Charmant, A.G. Orpen, I.D. Williams, Science 283 (1999) 1148–1150.
[15] P. Horcajada, S. Surblé, C. Serre, D.-Y. Hong, Y.-K. Seo, J.-S. Chang, J.-M. Grenèche, I. Margiolaki, G. Férey, Chem. Commun. (2007) 2820.
[16] G. Ferey, C. Serre, C. Mellot-Draznieks, F. Millange, S. Surble, J. Dutour, I. Margiolaki, Angew. Chem. Int. Ed. 43 (2004) 6296–6301.
[17] K. Schlichte, T. Kratzke, S. Kaskel, Micropor. Mesopor. Mater. 73 (2004) 81–88.
[18] J.W. Han, C.L. Hill, J. Am. Chem. Soc. 129 (2007) 15094–15095.
[19] A. Dhakshinamoorthy, M. Alvaro, H. Garcia, ChemCatChem 2 (2010) 1438–1443.
[20] A. Dhakshinamoorthy, M. Alvaro, H. Garcia, Adv. Synth. Catal. 352 (2010) 171–177.
[21] E. Pérez-Mayoral, J. Čejka, ChemCatChem 3 (2011) 157–159.
[22] Y.-K. Seo, G. Hundal, I.T. Jang, Y.K. Hwang, C.-H. Jun, J.-S. Chang, Micropor. Mesopor. Mater. 119 (2009) 331–337.
[23] J.W. Yoon, Y.-K. Seo, Y.K. Hwang, J.-S. Chang, H. Leclerc, S. Wuttke, P. Bazin, A. Vimont, M. Daturi, E. Bloch, P.L. Llewellyn, C. Serre, P. Horcajada, J.-M. Grenèche, A.E. Rodrigues, G. Férey, Angew. Chem. Int. Ed. 49 (2010) 5949–5952.
[24] B. Gil, S.I. Zones, S.J. Hwang, M. Bejblova, J. Čejka, J. Phys. Chem. C 112 (2008) 2997–3008.
[25] B. Gil, personal communication.
[26] L. Grajciar, O. Bludsky, P. Nachtigall, J. Phys. Chem. Lett. 1 (2010) 3354–3359.
[27] A. Zukal, H. Šiklová, J. Čejka, Langmuir 24 (2008) 9837–9842.
[28] N. Žilková, M. Bejblová, B. Gil, S.I. Zones, A. Burton, C.Y. Chen, Z. Musilová-Pavlačková, G. Košová, J. Čejka, J. Catal. 266 (2009) 79–91.
[29] B. Gil, K. Mierzyńska, M. Szczerbińska, J. Datka, Micropor. Mesopor. Mater. 99 (2007) 328–333.